PROCEEDINGS OF SCIENCE

Spin correlations in top pair with di-gamma production at NLO+PS

Rikkert Frederix[*†]
Physik Department T31, Technische Universität München, James-Franck-Str. 1, D-85748 Garching, Germany
E-mail: rikkert.frederix@tum.de

In this talk an interface is presented between the multi-purpose next-to-leading-order Monte Carlo tool MADGRAPH5_AMC@NLO and the automated one-loop amplitude generator GOSAM. As a phenomenological application of this work, the interface is used to make predictions for the $t\bar{t}H$ and $t\bar{t}\gamma\gamma$ processes at the 13 TeV LHC. The differences between these two processes is studied, focussing in particular on observables that are sensitive to the polarisation of the top quarks.
This talk is based on Ref. [1].

Fourth Annual Large Hadron Collider Physics
13-18 June 2016
Lund, Sweden

*Speaker.
†I would like to thank H. van Deurzen, V. Hirschi, G. Luisoni, P. Mastrolia and G. Ossola for collaboration on this work.

1. Introduction

The LHC is collecting data at an energy scale never explored before. Recently, the first results from the Run II have been presented, albeit, so far, without any convincing signs of signatures beyond the SM. Multi-purpose tools at NLO accuracy [2, 3, 4] are of fundamental importance as they can provide accurate and precise results for most interesting SM process and beyond. To assess the reliability of the results, it is important to be able to connect various external modules to these tools to validate the default usage. Furthermore, these external modules might focus in solving a single complicated task, and could be developed to perform this task at utmost efficiency.

With these ideas in mind, in this talk an interface between the MADGRAPH5_AMC@NLO framework [2] and the GOSAM one-loop amplitude provider [5] is presented.

We apply the novel framework MADGRAPH5_AMC@NLO + GOSAM to compute the NLO corrections to the signal process, $pp \to t\bar{t}H$ with $H \to \gamma\gamma$, and its irreducible background $pp \to t\bar{t}\gamma\gamma$. We decay the top quarks keeping track of spin correlations, and match the calculation to a parton shower. The signal process is of importance in the extraction of the top quark Yukawa coupling and has been of interest in several recent studies, both at LO [6, 7, 8, 9] and NLO [10, 11, 12].

2. The interface between MADGRAPH5_AMC@NLO and GOSAM

The MADGRAPH5_AMC@NLO code [2] is a multi-purpose tool that allows for predictions for cross sections and differential distributions for processes at particle colliders. It is not based on a predetermined library of available processes, rather it constructs the requested process from lower level building blocks, i.e. the Feynman rules in the form of an UFO model file [13, 14]. Using these building blocks it generates all the Feynman diagrams in the form of helicity amplitudes. At tree level this is rather straight-forward [15], while for the one-loop amplitudes the dedicated package MADLOOP [16, 17, 18, 19, 20, 2] is used by default. The divergences present in the virtual corrections are analytically cancelled against the divergences coming from the (numerical) phase-space integration in the real-emission radiative corrections using the FKS subtraction method [21, 22]. Finally, the MC@NLO technique [23] is used to match the fixed order predictions to parton showers [24, 25, 26, 27].

The main idea that distinguishes the GOSAM framework [5] from other codes for the automated generation of one-loop amplitudes, and in particular MADLOOP, is the combined use of automated diagrammatic generation and algebraic manipulation in $d = 4-2\varepsilon$ dimensions. Helicity amplitudes are generated via Feynman diagrams and are algebraically manipulated and cast in the most appropriate output [28, 29, 30, 31, 32, 33]. After the generation of all contributing diagrams, the virtual corrections are evaluated using the integrand reduction via Laurent expansion [34], provided by NINJA [35, 36], or the d-dimensional integrand-level reduction method [17, 37, 38], as implemented in SAMURAI [39, 40]. Alternatively, the tensorial decomposition provided by GOLEM [41, 42, 43] is also available.

The interface between GOSAM and MADGRAPH5_AMC@NLO is based on the Binoth-Les Houches Accord as defined in [44]. This interface envisages cross talk between GOSAM and MADGRAPH5_AMC@NLO at two stages. During the first stage an order file is written by MADGRAPH5_AMC@NLO that request the generation of the virtual amplitudes for the process requested by the user. This also sets the numerical values of all the input parameters that do not change point-by-point in the phase-space, such that an optimized code can be generated. This order file is read by GoSAM which, if it is able to provide the requested virtual matrix elements, writes out a contract file. An example for the order and contract files for the $t\bar{t}\gamma\gamma$ process is shown in Fig. 1. The second stage of the interface is that after the amplitudes are generated, the two codes are linked together and the phase-space point as well as the parameters that depend on the phase-space point (i.e. α_s and the renormalisation scale) are transferred to GoSAM, which returns the coefficients of the double and single poles (in $d = 4-2\varepsilon$) as well as the finite part of the virtual corrections.

```
#OLE_order written by MadGraph5_aMC@NLO

MatrixElementSquareType CHaveraged
CorrectionType          QCD
IRregularisation        CDR
AlphasPower             2
AlphaPower              2
NJetSymmetrizeFinal     Yes
ModelFile               ./param_card.dat
Parameters              alpha_s


# process
21 21 -> 22 22 6 -6
2 -2 -> 22 22 6 -6
1 -1 -> 22 22 6 -6
-2 2 -> 22 22 6 -6
-1 1 -> 22 22 6 -6
```

```
# vim: syntax=olp
#@OLP GoSam 2.0.0
#@IgnoreUnknown True
#@IgnoreCase False
#@SyntaxExtensions
MatrixElementSquareType CHaveraged | OK
CorrectionType QCD | OK
IRregularisation CDR | OK
AlphasPower 2 | OK
AlphaPower 2 | OK
NJetSymmetrizeFinal Yes | OK #Ignored
ModelFile ./param_card.dat | OK
Parameters alpha_s | OK
21 21 -> 22 22 6 -6 | 1 2
2 -2 -> 22 22 6 -6 | 1 0
1 -1 -> 22 22 6 -6 | 1 3
-2 2 -> 22 22 6 -6 | 1 1
-1 1 -> 22 22 6 -6 | 1 4
```

Figure 1: Example of order file (left) and contract file (right).

The MADGRAPH5_AMC@NLO and GoSAM codes can be downloaded from the following URLs:

MADGRAPH5_AMC@NLO: `http://amcatnlo.cern.ch`

GoSAM: `http://gosam.hepforge.org`

The interface is available starting from MADGRAPH5_AMC@NLO version 2.3.2.2, and has been tested for numerous processes both at the level of single phase-space points as well as for (partially) integrated results. Excellent agreement has been found between using virtual corrections from the build-in MADLOOP module and the GoSAM code through the BLHA.

3. Application to $t\bar{t}H$ and $t\bar{t}\gamma\gamma$

As an application of the newly created interface, we apply it to NLO predictions for the $t\bar{t}H$ and $t\bar{t}\gamma\gamma$ processes at the 13 TeV LHC. The latter is the irreducible background to the $t\bar{t}H$ process in which the Higgs decays to photons, which is the decay mode we focus upon. Both the top and anti-top quarks are decayed semi-leptonically, keeping track of spin-correlation effects through the use of MADSPIN [45, 46]. The generated events are showered and hadronised using PYTHIA 8.2 with its default parameters, but with the underlying event turned off.

PoS(LHCP2016)163

The results presented here are computed using the following setup. The masses of the top quark and Higgs and Z bosons are set to $m_t = 173.2$ GeV and $m_H = 125$ GeV and $m_Z = 91.1876$ GeV, repectively. The value of the electroweak coupling is set to its low energy limit $\alpha_{EW}^{-1} = 137.0$, which is the preferred choice for processes with tagged photons. The value of the Fermi constant to $G_F = 1.16639 \cdot 10^{-5}$ GeV^{-2}, which, together with the mass of the Z boson specified above, fixes the electroweak scheme. We use the value of $\alpha_s(m_Z)$ and parton luminosities as provided by the NLO CT10 PDF set [47]. The central values of the renormalisation and factorisation scales are set to $\mu_R = \mu_F = \mu_0$ with

$$\mu_0 = \frac{\hat{H}_T}{2} = \frac{1}{2}\left(\sum_i \sqrt{m_i^2 + p_{T,i}^2}\right), \tag{3.1}$$

where i runs over the two top quarks, the two photons (in the case of $t\bar{t}\gamma\gamma$) or the Higgs boson (in the case of $t\bar{t}H$) and the possible final state parton present in the real-emission corrections.

The analysis cuts are designed to increase the signal over the background, but are by no means optimised to maximise efficiency. We use MC truth information to select the two photons from the Higgs decay (or the two hard photons in the $t\bar{t}\gamma\gamma$ process) and they are required to be isolated following the smooth-cone procedure [48] with parameters, $R_\gamma < 0.4$, $n = 1.0$ and $\varepsilon_\gamma = 1.0$. Furthermore, we apply an isolation radius between the two photons $R_{\gamma\gamma} = 0.4$. To pass the selection, the isolated photons have to fulfill

$$p_{T,\gamma} > 20\text{ GeV}, \quad |\eta_\gamma| < 2.5, \quad 123\text{ GeV} < m_{\gamma\gamma} < 129\text{ GeV}, \tag{3.2}$$

where the invariant mass requirement selects a window around the Higgs boson mass. We require the events to have at least two opositely charged leptons and at least two b-jets coming from the top and anti-top decays. Also here MC truth information is used to select the correct leptons and B mesons among the event record. The jets are defined by clustering all stable hadrons and photons, but excluding the two photons selected using Eq. (3.2), using the anti-k_T algortithm as implemented in the code FASTJET [49, 50, 51], with

$$\Delta R = 0.4, \quad p_{T,j} > 20\text{ GeV}, \quad |\eta_j| < 4.7. \tag{3.3}$$

The b-jets are defined to be jets containing at least one lowest lying B meson. The leptons are selected requiring

$$p_{T,l^\pm} > 10\text{ GeV}, \quad |\eta_{l^\pm}| < 2.7. \tag{3.4}$$

In the presence of these analysis cuts, we obtain the cross-sections reported in Table 1.

As can be seen from this table, with the simple set of cuts specified above, the cross sections for the background and signal are of similar order, although both are rather small. Hence, getting even the total cross section with the upcoming Run II LHC data will be rather challenging. Nevertheless, we will now show some differential distributions, pointing out differences between the signal and background processes. This is not something that is forseen to measurable with LHC data, but rather to point out some interesting theoretical features in the differences between $t\bar{t}H$ and $t\bar{t}\gamma\gamma$. Therefore, we also assume a 100% top tagging efficiency; in fact, for observables that require the specific top quark momentum, we use the momentum of the top quark in the PYTHIA event file record just before it decays.

$\sqrt{s} = 13$ TeV	$pp \to t\bar{t}H,\, H \to \gamma\gamma$	$pp \to t\bar{t}\gamma\gamma$
LO [pb]	$8.84(2) \cdot 10^{-7}\ {}^{+27\%}_{-20\%}\ {}^{+10\%}_{-11\%}$	$1.442(2) \cdot 10^{-7}\ {}^{+25\%}_{-18\%}\ {}^{+10\%}_{-12\%}$
NLO [pb]	$11.77(5) \cdot 10^{-7}\ {}^{+6\%}_{-8\%}\ {}^{+11\%}_{-12\%}$	$2.175(7) \cdot 10^{-7}\ {}^{+10\%}_{-10\%}\ {}^{+10\%}_{-11\%}$
K-factor	1.33(1)	1.51(1)

Table 1: Cross sections in picobarns, at a center-of-mass energy of $\sqrt{s} = 13$ TeV and in the presence of the analysis cuts described in the text. The two sets of uncertainties following the cross-section correspond to the scale and PDF variations respectively.

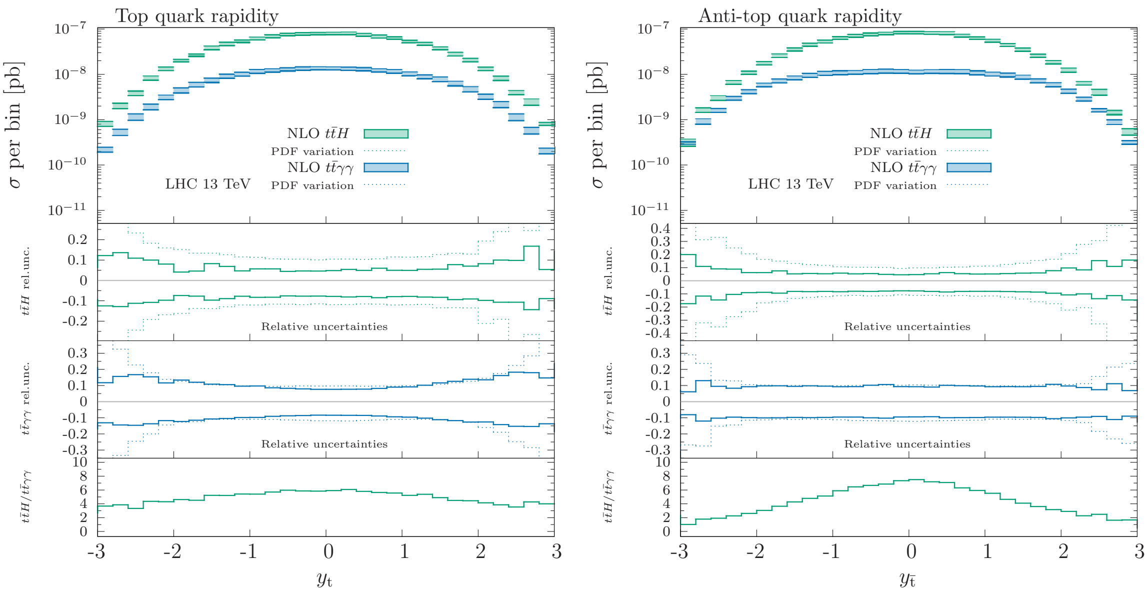

Figure 2: Rapidity distribution of the top quark (left) and anti-top quark (right).

The first observables we consider are the top and anti-top quark rapidities, shown in fig. 2. The difference in shape in the broadness of the distribution is particular visible for the $t\bar{t}\gamma\gamma$ background process. This is a thoroughly studied feature, known as the charge asymmetry, which is usually quantified as

$$A^{C}_{t\bar{t}} = \frac{\sigma\,(\Delta|y| > 0) - \sigma\,(\Delta|y| < 0)}{\sigma\,(\Delta|y| > 0) + \sigma\,(\Delta|y| < 0)}\,, \tag{3.5}$$

where $\Delta|y| = |y_t| - |y_{\bar{t}}|$. For inclusive top-pair production at the LHC this observable is positive [52]. However, the presence of photons reverses the sign of the $A^{C}_{t\bar{t}}$ already at the tree level [53], and is also clearly visible in the plots. As expected, the charge assymetry for the signal process, $t\bar{t}H$, is much smaller.

The second observable that is of interest is the angle between the two leptons coming from the top and anti-top quark decays. This angle is very sensitive to the spin correlations between the top and anti-top quarks [54, 55, 56]. The most straight-forward possibility of defining the angle θ_{ll} is in the laboratory frame, but other frames [55] are commonly used as well. We will consider the

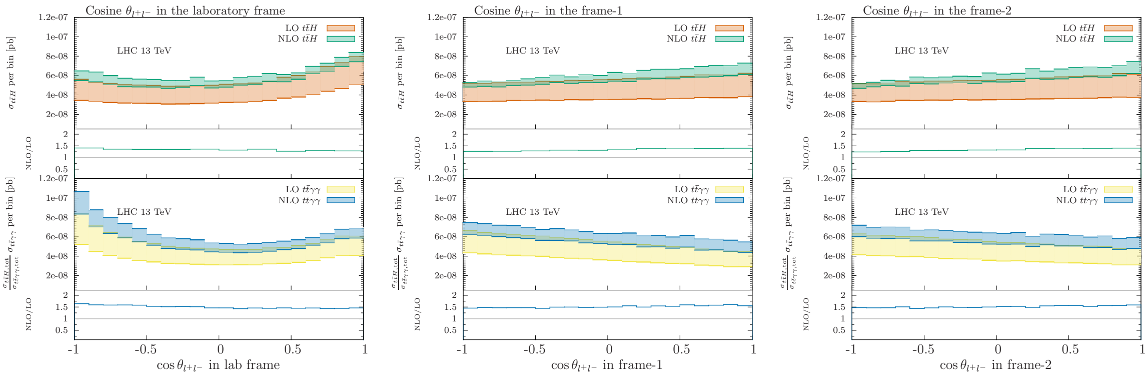

Figure 3: A comparison of LO versus NLO $\cos\theta_{ll}$ distribution for the signal ($t\bar{t}H$) and background ($t\bar{t}\gamma\gamma$) processes in the three frames. The $t\bar{t}\gamma\gamma$ prediction is normalized to the $t\bar{t}H$ inclusive cross-section.

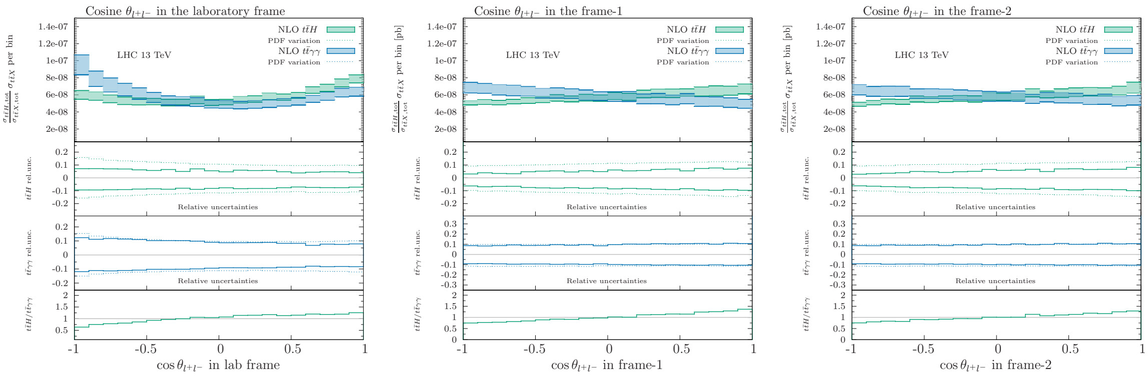

Figure 4: A comparison for the $\cos\theta_{ll}$ distribution for the signal ($t\bar{t}H$) and background ($t\bar{t}\gamma\gamma$) processes in the three frames. The $t\bar{t}\gamma\gamma$ prediction is normalized to the $t\bar{t}H$ inclusive cross-section.

following frames:

- *lab frame*: the laboratory frame,
- *frame-1*: the Lorentz boosts to bring t and $\bar{t}$ separately at rest are defined with respect to the $t\bar{t}$-pair center-of-mass frame,
- *frame-2*: the Lorentz boosts to bring t and $\bar{t}$ separately at rest are defined with respect to the lab-frame.

For the latter two frames, we define θ_{ll} to be the angle between the direction of flight of l^+, measured in frame where the *top quark* is at rest, and the direction of flight of l^-, measured in the frame where the *anti-top quark* is at rest.

In figs. 3 and 4 we show the behaviour of $\cos\theta_{ll}$ for the three frames as a comparison of LO versus NLO and signal versus background, respectively. As can be understood from fig. 3, the NLO corrections only mildly change the shape of the distributions. From the lowest inset of the plots in fig. 4 it can be concluded that there is a clear difference in spin correlations between the signal and the background irrespective of the reference frame, but also that frame-1 shows the largest effect.

4. Conclusions

In this talk, a fully flexible interface between the MADGRAPH5_AMC@NLO and GOSAM codes has been presented. It has been tested for a multitute of processes both at the level of single phase-space points as well as (semi-)inclusive observables. The interface is available in the public versions of the relevant codes.

The newly interface has been applied to the $t\bar{t}H$ and $t\bar{t}\gamma\gamma$ processes, pointing out some interesting features and differences between the two, in particular regarding the top quark charge asymmetry and the spin correlation effects between the top quarks.

Now that this interface is available, a fair comparison between MADLOOP and GOSAM can be made. For the processes studied in this work ($t\bar{t}H$ and $t\bar{t}\gamma\gamma$), MADLOOP outperforms GOSAM in terms of speed at generation time as well as run time, and with negligible differences observed in terms of stability. However, it is likely that this is will be very different for other processes, and we therefore recommend that a user should check which of the one-loop matrix-element providers renders his/her NLO calculation the quickest.

Acknowledgements

The speaker is supported by the Alexander von Humboldt Foundation, in the framework of the Sofja Kovalevskaja Award Project "Event Simulation for the Large Hadron Collider at High Precision".

References

[1] H. van Deurzen, R. Frederix, V. Hirschi, G. Luisoni, P. Mastrolia and G. Ossola, Eur. Phys. J. C **76** (2016) no.4, 221 doi:10.1140/epjc/s10052-016-4048-2 [arXiv:1509.02077 [hep-ph]].

[2] J. Alwall *et al.*, JHEP **1407** (2014) 079 doi:10.1007/JHEP07(2014)079 [arXiv:1405.0301 [hep-ph]].

[3] T. Gleisberg, S. Hoeche, F. Krauss, M. Schonherr, S. Schumann, F. Siegert and J. Winter, JHEP **0902** (2009) 007 doi:10.1088/1126-6708/2009/02/007 [arXiv:0811.4622 [hep-ph]].

[4] S. Alioli, P. Nason, C. Oleari and E. Re, JHEP **1006** (2010) 043 doi:10.1007/JHEP06(2010)043 [arXiv:1002.2581 [hep-ph]].

[5] G. Cullen *et al.*, Eur. Phys. J. C **74** (2014) no.8, 3001 doi:10.1140/epjc/s10052-014-3001-5 [arXiv:1404.7096 [hep-ph]].

[6] S. Biswas, R. Frederix, E. Gabrielli and B. Mele, JHEP **1407** (2014) 020 doi:10.1007/JHEP07(2014)020 [arXiv:1403.1790 [hep-ph]].

[7] A. Denner, R. Feger and A. Scharf, JHEP **1504** (2015) 008 doi:10.1007/JHEP04(2015)008 [arXiv:1412.5290 [hep-ph]].

[8] S. P. Amor dos Santos *et al.*, Phys. Rev. D **92** (2015) no.3, 034021 doi:10.1103/PhysRevD.92.034021 [arXiv:1503.07787 [hep-ph]].

[9] M. R. Buckley and D. Goncalves, Phys. Rev. Lett. **116** (2016) no.9, 091801 doi:10.1103/PhysRevLett.116.091801 [arXiv:1507.07926 [hep-ph]].

[10] A. Kardos and Z. TrÃşcsÃąnyi, Nucl. Phys. B **897** (2015) 717 doi:10.1016/j.nuclphysb.2015.05.032 [arXiv:1408.0278 [hep-ph]].

[11] A. Denner and R. Feger, JHEP **1511** (2015) 209 doi:10.1007/JHEP11(2015)209 [arXiv:1506.07448 [hep-ph]].

[12] F. Maltoni, D. Pagani and I. Tsinikos, JHEP **1602** (2016) 113 doi:10.1007/JHEP02(2016)113 [arXiv:1507.05640 [hep-ph]].

[13] C. Degrande, C. Duhr, B. Fuks, D. Grellscheid, O. Mattelaer and T. Reiter, Comput. Phys. Commun. **183** (2012) 1201 doi:10.1016/j.cpc.2012.01.022 [arXiv:1108.2040 [hep-ph]].

[14] A. Alloul, N. D. Christensen, C. Degrande, C. Duhr and B. Fuks, Comput. Phys. Commun. **185** (2014) 2250 doi:10.1016/j.cpc.2014.04.012 [arXiv:1310.1921 [hep-ph]].

[15] J. Alwall, M. Herquet, F. Maltoni, O. Mattelaer and T. Stelzer, JHEP **1106** (2011) 128 doi:10.1007/JHEP06(2011)128 [arXiv:1106.0522 [hep-ph]].

[16] V. Hirschi, R. Frederix, S. Frixione, M. V. Garzelli, F. Maltoni and R. Pittau, JHEP **1105** (2011) 044 doi:10.1007/JHEP05(2011)044 [arXiv:1103.0621 [hep-ph]].

[17] G. Ossola, C. G. Papadopoulos and R. Pittau, Nucl. Phys. B **763** (2007) 147 doi:10.1016/j.nuclphysb.2006.11.012 [hep-ph/0609007].

[18] G. Ossola, C. G. Papadopoulos and R. Pittau, JHEP **0803** (2008) 042 doi:10.1088/1126-6708/2008/03/042 [arXiv:0711.3596 [hep-ph]].

[19] G. Ossola, C. G. Papadopoulos and R. Pittau, JHEP **0805** (2008) 004 doi:10.1088/1126-6708/2008/05/004 [arXiv:0802.1876 [hep-ph]].

[20] F. Cascioli, P. Maierhofer and S. Pozzorini, Phys. Rev. Lett. **108** (2012) 111601 doi:10.1103/PhysRevLett.108.111601 [arXiv:1111.5206 [hep-ph]].

[21] S. Frixione, Z. Kunszt and A. Signer, Nucl. Phys. B **467** (1996) 399 doi:10.1016/0550-3213(96)00110-1 [hep-ph/9512328].

[22] R. Frederix, S. Frixione, F. Maltoni and T. Stelzer, JHEP **0910** (2009) 003 doi:10.1088/1126-6708/2009/10/003 [arXiv:0908.4272 [hep-ph]].

[23] S. Frixione and B. R. Webber, JHEP **0206** (2002) 029 doi:10.1088/1126-6708/2002/06/029 [hep-ph/0204244].

[24] T. Sjostrand, S. Mrenna and P. Z. Skands, JHEP **0605** (2006) 026 doi:10.1088/1126-6708/2006/05/026 [hep-ph/0603175].

[25] G. Corcella, I. G. Knowles, G. Marchesini, S. Moretti, K. Odagiri, P. Richardson, M. H. Seymour and B. R. Webber, JHEP **0101** (2001) 010 doi:10.1088/1126-6708/2001/01/010 [hep-ph/0011363].

[26] T. SjÃűstrand *et al.*, Comput. Phys. Commun. **191** (2015) 159 doi:10.1016/j.cpc.2015.01.024 [arXiv:1410.3012 [hep-ph]].

[27] M. Bahr *et al.*, Eur. Phys. J. C **58** (2008) 639 doi:10.1140/epjc/s10052-008-0798-9 [arXiv:0803.0883 [hep-ph]].

[28] B. Chokoufe Nejad, T. Hahn, J.-N. Lang and E. Mirabella, J. Phys. Conf. Ser. **523** (2014) 012050 doi:10.1088/1742-6596/523/1/012050 [arXiv:1310.0274 [hep-ph]].

[29] P. Nogueira, J. Comput. Phys. **105** (1993) 279. doi:10.1006/jcph.1993.1074

[30] J. A. M. Vermaseren, math-ph/0010025.

[31] T. Reiter, Comput. Phys. Commun. **181** (2010) 1301 doi:10.1016/j.cpc.2010.01.012 [arXiv:0907.3714 [hep-ph]].

[32] G. Cullen, M. Koch-Janusz and T. Reiter, Comput. Phys. Commun. **182** (2011) 2368 doi:10.1016/j.cpc.2011.06.007 [arXiv:1008.0803 [hep-ph]].

[33] J. Kuipers, T. Ueda, J. A. M. Vermaseren and J. Vollinga, Comput. Phys. Commun. **184** (2013) 1453 doi:10.1016/j.cpc.2012.12.028 [arXiv:1203.6543 [cs.SC]].

[34] P. Mastrolia, E. Mirabella and T. Peraro, JHEP **1206** (2012) 095 Erratum: [JHEP **1211** (2012) 128] doi:10.1007/JHEP11(2012)128, 10.1007/JHEP06(2012)095 [arXiv:1203.0291 [hep-ph]].

[35] H. van Deurzen, G. Luisoni, P. Mastrolia, E. Mirabella, G. Ossola and T. Peraro, JHEP **1403** (2014) 115 doi:10.1007/JHEP03(2014)115 [arXiv:1312.6678 [hep-ph]].

[36] T. Peraro, Comput. Phys. Commun. **185** (2014) 2771 doi:10.1016/j.cpc.2014.06.017 [arXiv:1403.1229 [hep-ph]].

[37] R. K. Ellis, W. T. Giele, Z. Kunszt and K. Melnikov, Nucl. Phys. B **822** (2009) 270 doi:10.1016/j.nuclphysb.2009.07.023 [arXiv:0806.3467 [hep-ph]].

[38] P. Mastrolia, G. Ossola, C. G. Papadopoulos and R. Pittau, JHEP **0806** (2008) 030 doi:10.1088/1126-6708/2008/06/030 [arXiv:0803.3964 [hep-ph]].

[39] P. Mastrolia, G. Ossola, T. Reiter and F. Tramontano, JHEP **1008** (2010) 080 doi:10.1007/JHEP08(2010)080 [arXiv:1006.0710 [hep-ph]].

[40] H. van Deurzen, Acta Phys. Polon. B **44** (2013) no.11, 2223. doi:10.5506/APhysPolB.44.2223

[41] T. Binoth, J.-P. Guillet, G. Heinrich, E. Pilon and T. Reiter, Comput. Phys. Commun. **180** (2009) 2317 doi:10.1016/j.cpc.2009.06.024 [arXiv:0810.0992 [hep-ph]].

[42] G. Cullen, J. P. Guillet, G. Heinrich, T. Kleinschmidt, E. Pilon, T. Reiter and M. Rodgers, Comput. Phys. Commun. **182** (2011) 2276 doi:10.1016/j.cpc.2011.05.015 [arXiv:1101.5595 [hep-ph]].

[43] J. P. Guillet, G. Heinrich and J. F. von Soden-Fraunhofen, Comput. Phys. Commun. **185** (2014) 1828 doi:10.1016/j.cpc.2014.03.009 [arXiv:1312.3887 [hep-ph]].

[44] T. Binoth *et al.*, Comput. Phys. Commun. **181** (2010) 1612 doi:10.1016/j.cpc.2010.05.016 [arXiv:1001.1307 [hep-ph]].

[45] S. Frixione, E. Laenen, P. Motylinski and B. R. Webber, JHEP **0704** (2007) 081 doi:10.1088/1126-6708/2007/04/081 [hep-ph/0702198 [HEP-PH]].

[46] P. Artoisenet, R. Frederix, O. Mattelaer and R. Rietkerk, JHEP **1303** (2013) 015 doi:10.1007/JHEP03(2013)015 [arXiv:1212.3460 [hep-ph]].

[47] J. Gao *et al.*, Phys. Rev. D **89** (2014) no.3, 033009 doi:10.1103/PhysRevD.89.033009 [arXiv:1302.6246 [hep-ph]].

[48] S. Frixione, Phys. Lett. B **429** (1998) 369 doi:10.1016/S0370-2693(98)00454-7 [hep-ph/9801442].

[49] M. Cacciari and G. P. Salam, Phys. Lett. B **641** (2006) 57 doi:10.1016/j.physletb.2006.08.037 [hep-ph/0512210].

[50] M. Cacciari, G. P. Salam and G. Soyez, JHEP **0804** (2008) 063 doi:10.1088/1126-6708/2008/04/063 [arXiv:0802.1189 [hep-ph]].

[51] M. Cacciari, G. P. Salam and G. Soyez, Eur. Phys. J. C **72** (2012) 1896 doi:10.1140/epjc/s10052-012-1896-2 [arXiv:1111.6097 [hep-ph]].

PoS(LHCP2016)163

[52] J. H. Kuhn and G. Rodrigo, Phys. Rev. D **59** (1999) 054017 doi:10.1103/PhysRevD.59.054017 [hep-ph/9807420].

[53] J. A. Aguilar-Saavedra, E. ÃĄlvarez, A. Juste and F. Rubbo, JHEP **1404** (2014) 188 doi:10.1007/JHEP04(2014)188 [arXiv:1402.3598 [hep-ph]].

[54] W. Bernreuther, A. Brandenburg, Z. G. Si and P. Uwer, Phys. Rev. Lett. **87** (2001) 242002 doi:10.1103/PhysRevLett.87.242002 [hep-ph/0107086].

[55] W. Bernreuther, A. Brandenburg, Z. G. Si and P. Uwer, Nucl. Phys. B **690** (2004) 81 doi:10.1016/j.nuclphysb.2004.04.019 [hep-ph/0403035].

[56] W. Bernreuther and Z. G. Si, Nucl. Phys. B **837** (2010) 90 doi:10.1016/j.nuclphysb.2010.05.001 [arXiv:1003.3926 [hep-ph]].